One-step impedimetric NT-proBNP aptasensor targeting cardiac insufficiency in artificial saliva

Waralee Ruankham, Isaac Aarón Morales Frías, Kamonrat Phopin, Tanawut Tantimongcolwat, Joan Bausells, Nadia Zine, Abdelhamid Errachid, Abdelhamid Errachid El Salhi

One-step impedimetric NT-proBNP aptasensor targeting cardiac insufficiency in artificial saliva

Waralee Ruankham[a], Isaac Aarón Morales Frías[b], Kamonrat Phopin[a,c], Tanawut Tantimongcolwat[a], Joan Bausells[d], Nadia Zine[b], Abdelhamid Errachid[b,*]

[a]Center for Research and Innovation, Faculty of Medical Technology, Mahidol University, Bangkok, 10700, Thailand.

[b]Institut des Sciences Analytiques (ISA), Université Claude Bernard Lyon-1, Lyon, 69100, France.

[c]Department of Clinical Microbiology and Applied Technology, Faculty of Medical Technology, Mahidol University, Bangkok, 10700, Thailand.

[d]Instituto de Microelectrónica de Barcelona (IMB-CNM-CSIC), Campus Universitat Autònoma de Barcelona (UAB), Barcelona, 08193, Spain

[*]Corresponding author: A.E.

Email: abdelhamid.errachid@univ-lyon1.fr Phone: +33 (0)4 37 42 35 60, +33 (0)6 25 18 64 34

Abstract

Currently, sensitive and accurate approaches for diagnosis, rapid assessment, and cardiac biomarker monitoring in patients with heart failure are needed. In this context, the advantages of aptamers over traditional antibodies have been employed to fabricate a single-step impedimetric N-terminal pro b-type natriuretic peptide (NT-proBNP)-modified gold microelectrode array. The development of an electrochemical aptasensing platform was based on the coimmobilization of alkanethiol self-assembled monolayers and amine-terminated aptamer that specifically recognised cardiac NT-proBNP protein resulting in charge electron transfer. Electroimpedimetric signals of the sensor were observed to be linear to the NT-proBNP concentrations in the range of $5.0x10^{-3}$ to 1.0 pg mL^{-1} (R^2 = 0.9624), while achieving a low detection limit of $5.0x10^{-3}$ pg mL^{-1}. Clinically relevant detection levels for NT-proBNP are achieved in a simple, rapid, and label-free measurement using artificial saliva, which was highlighted to be specific, regenerative, and selective over potential interferers occurring during the processes of cardiac insufficiency, Therefore, the novel NT-proBNP aptasensor is a promising point-of-care tool exhibiting safe, noninvasive, affordable, and non-prescription home use accessible to overcome the limitations associated with conventional ELISA and previous aptasensing.

Keywords: N-terminal pro b-type natriuretic peptide; Label-free aptasensor; Electrochemical impedance spectroscopy; Cardiac insufficiency; Artificial saliva

1. Introduction

The prevalence and incidence of cardiac insufficiency, commonly known as heart failure, have been reported that over 64 million people of all ages, especially a constantly increasing proportion of the aging population aged older than 65 are affected by some form of heart failure worldwide [1, 2]. The untreated and poor prognosis of common cardiovascular diseases can be aggressive, leading to the global burden of mortality, morbidity, hospitalization, and healthcare economic system [3-5]. Natriuretic peptide, is a hormonal substance secreted by the heart to help transport blood throughout the body. This hormone consists of brain natriuretic peptide (BNP) and non-active N-terminal pro b-type natriuretic peptide (NT-proBNP) which are released in the bloodstream regarding changes in pressure inside the heart [6, 7]. NT-proBNP levels cut off higher than 450.0 pg mL^{-1} is indicated that patients are high-risk individuals for major cardiovascular conditions. Furthermore, elevated levels of both BNP and NT-proBNP substances are considered a status for patients with heart failure at a cut-off point of 900.0 pg mL^{-1} [8, 9]. Currently, clinical findings and routine diagnosis are relied on benchtop-based instruments which are expensive devices, time-consuming, and require specially trained personnel to operate. Due to these limitations and invasive investigation, sensitive and reliable electrochemical biosensors have widely drawn attention for helping diagnosis, accessing the severity of condition, monitoring heart failure, and managing therapeutics [10-12].

Aptamers are three-dimensional structures of artificial nucleic acids which provide several advantages over antibodies, i.e., high affinity, less immunogenicity, chemical synthesis, thermal tolerance, pH stability, and low cost [13, 14]. They can thus be easily functionalized with several substances to perform specific molecular recognition complexes for various biosensing platforms, e.g., photoelectrochemical aptasensing of prostate-specific antigen (PSA) [15] and carcinoembryonic antigen

(CEA) [16]. The use of modified aptamer also allows academic and industrious researchers to avoid the expense of high-cost devices, and reduce the impact of ambient disturbances. Recent studies have been successfully applied in various applications, for example, a near-infrared (NIR)-activated PEC aptasensing [17] and an all-in-one paper-based analytical device (PAD) [18] for CEA detection on a portable smartphone, which translates tremendous know-how from clinical laboratories toward on-site determination. Considering the advantages of impedance and aptamer, aptasensors were conducted for the detection of cardiac biomarkers by electrochemical approaches. Electrochemical impedance spectroscopy (EIS)-based aptasensors have displayed excellent potentials for multiplexed analysis and on-site detection of a variety of analytes with fast response, high sensitivity and specificity, cost-effective fabrication, and simple operation [19-21].

In an attempt to quantify the level of NT-proBNP, different aptasensors have been developed by focusing on transduced signal amplification, improved detection limit, and efficient probe immobilization. The well-established NT-proBNP aptamer-based sandwich assay with its highly specific aptamer coated on magnetic beads and impressive miniaturization was integrated through the usage of microfluidic chemiluminescent platforms. This practicality was capable of simultaneously detecting NT-proBNP in clinical samples and represented a convenient alternative towards point-of-care diagnostics for cardiac insufficiency [22]. Moreover, an aptamer-NT-ProBNP-antibody sandwich pattern was constructed on a microelectrode surface by using zeolite-iron oxide (ZEO-IO) nanocomposite to detect the level of NT-ProBNP in serum. However, the above sensor still further needed optimization to counteract some limitations due to an oxide base material [23]. The majority of aptasensors that have been developed with several paradigms are limited for the detection of NT-proBNP and none utilizing the potential benefits of regeneration within the physiological range down to picomolar has been

reported. To the best of our knowledge, there is no previous study that explores the trace amounts of NT-proBNP in saliva matrix by single-step aptasensing platform.

Herein, a single-step impedimetric NT-proBNP aptasensors based on gold microelectrode array for the detection of cardiac NT-proBNP biomarker. Coimmobilization of aminated aptamer and alkanethiol was constructed through amine-gold interaction. The enhance electrochemical response of NT-proBNP was determined based on CV and EIS using $[Fe(CN)_6]^{3-/4-}$ as redox couples. Moreover, the risk stratification threshold of trace NT-proBNP in human artificial saliva samples was reported for the first time, together with ultrasensitivity, high selectivity, strong stability, and good reusability. Therefore, this work highlighted a novel approach for the fabrication of simple, rapid, and reusable NT-proBNP aptasensor which could be a potential alternative device for diagnosis and monitoring of cardiac insufficiency over the limitations of traditional antibodies and ELISA method.

2. Materials and methods

2.1. Chemical and reagents

Human brain natriuretic peptide (proBNP) and N-terminal part of the BNP precursor proBNP (NT-proBNP) were obtained from HyTest (Turku, Finland). Published NT-proBNP aptamer [22, 24] was synthesized with a modification of the amine (NH_2) at the 5'-end (5'-NH_2-GGCAGGAAGACAAACAGGTCGTAGTGGAAACTGTCCACCGTAGACCGGTTATCTAGTGGTC TGTGGTGCTGT-3') from Microsynth (Balgach, Switzerland). Recombinant human interleukin 10 (IL-10) and tumor necrosis factor alpha (TNF-α) were purchased from R&D Systems (Minnesota, USA). UltraPure DNase/RNase-free distilled water was supplied from Thermo Fisher Scientific (Massachusetts, USA). FITC-conjugated rabbit polyclonal NT-proBNP antibody was provided from

Abbexa (Cambridge, UK). All reagents were analytical grade from Sigma-Aldrich (Darmstadt, Germany) unless otherwise stated.

2.2. Fabrication of the NT-proBNP-based aptasensor

Microelectrode array sensor is relied on four gold (Au) working microelectrodes, a platinum (Pt) counter microelectrode, and two internal Ag/AgCl reference microelectrodes, which was cleaned by a mixture of 25% hydrogen peroxide (H_2O_2) and 50.0 mM potassium hydroxide (KOH) [25]. 1.0 μM NH_2-terminated aptamer was performed heating and cooling step for the proper folding into its structure prior to coimmobilization with 1.0 mM 6-mercapto-1-hexanol (MCH) onto the pretreated microelectrode array at 4 °C overnight. The process of immobilizing the modified aptamer on the microelectrode array is illustrated in Fig. 1. Subsequently, the modified microelectrodes were washed with a solution of phosphate-buffered saline (PBS) for removing any unbound aptamers and excessive MCH. Finally, NT-proBNP solution was dropped onto the aptamer-functionalized microelectrodes with different concentrations for further experiments.

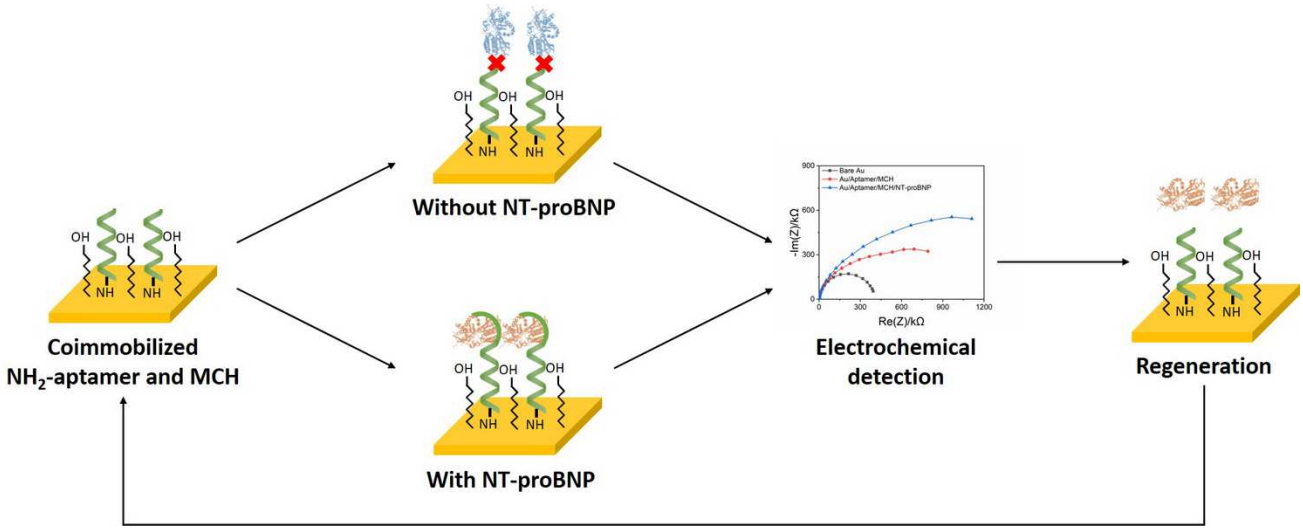

Fig. 1. Schematic view of the impedimetric aptasensor and the detection of NT-proBNP on the microelectrode array.

2.3. Characterization and performance of the build-up process for NT-proBNP aptasensor

Different chemical compositions of microelectrode surfaces were determined by a Nexus ThermoNicolet Fourier transform infrared (FTIR) system operated with OMNIC™ Series Software (Thermo Fisher Scientific, Massachusetts, USA), which was equipped with a high sensitivity liquid nitrogen cooled mercury-cadmium-telluride (MCT) detector and recorded at a resolution of 4 cm^{-1} with an accumulation of 256 scans. Moreover, contact angle measurement (CAM) was employed to investigate different coating layers of microelectrode surfaces by using a contact angle system OCA and analyzing with an enclosed SCA20 software (DataPhysics Instruments, Filderstadt, Germany). Fluorescence imaging was also provided to further confirm the presence of NT-proBNP-aptamer complexes onto the modified surfaces by EVOS M5000 Imaging System (Thermo Fisher Scientific, Massachusetts, USA).

Electrochemical measurements, including electrochemical impedance spectroscopy (EIS) and cyclic voltammetry (CV) were carried out through SP-200 potentiostat (BioLogic Science Instrument, Seyssinet-Pariset, France). Briefly, the functionalization of Au microelectrode array with NH_2-modified NT-proBNP aptamer was incubated with various concentrations of NT-proBNP at room temperature for 15 min. Afterward, the unbound NT-proBNP was eliminated by rinsing with PBS. The microelectrode array was electrochemically treated through oxidation and reduction cycling in an aqueous PBS solution containing an equimolar solution of 5.0 mM ferri-/ferrocyanide $[Fe(CN)_6]^{3-/4-}$ couples from −0.2 to +0.6 V with a scan rate of 50 mV/s. The EIS measurement was also conducted over a frequency range of 200 mHz−100 kHz and a potential of −0.4 V. Finally, the data of EIS were fitted by a Randles equivalent electrical circuit using $R_1+Q_2/(R_2+W_2)$, where R_1 is an electrolyte resistance and R_2 expresses a charge transfer resistance. W_2 is a Warburg impedance and Q_2 refers to a constant phase element. The data were visualized by the OriginLab software (OriginLab Corporation, Massachusetts, USA).

2.4. Application of NT-proBNP aptasensor in artificial saliva (AS)

According to a previous procedure [26], artificial saliva (AS) was implemented by dissolving 3.0 mg sodium phosphate dibasic (Na_2HPO_4), 3.0 mg anhydrous calcium chloride ($CaCl_2$), 2.0 mg potassium chloride (KCl), 2.0 mg sodium chloride (NaCl), 20.0 mg mucin, and 20.0 mg urea in 5.0 mL of deionized water. The mixture was sonicated homogeneously for 30 min, neutralized with 1.0 N sodium hydroxide (NaOH) to achieve a final pH of 7.2, and stored at −4 °C until use. To simulate a real saliva sample analysis, a standard addition method was performed. A constant volume (50.0 μL) of the unknown sample (represented by 1.0 pg mL^{-1} of NT-proBNP in AS) was spiked with the appropriate amount of 100.0 pg mL^{-1} stock solution to obtain the various concentrations of NT-proBNP (0, 1.0, 2.0, and 5.0 pg mL^{-1}) and then adjusted a final volume to 1.0 mL by adding PBS. The different concentrations of NT-proBNP in AS were analyzed to investigate the linearity of the aptasensor.

3. Results and discussion

3.1. Surface characterization of modified NT-proBNP aptamer and NT-proBNP

Characterization and interaction of the modified surface were verified by FTIR, CAM, and fluorescence imaging. After the Au microelectrode array was modified by NT-proBNP aptamer, absorbance peaks were observed at wavenumbers of 2927, 2854, and 1475 cm^{-1} (−CH_2); 3300 and 1664 cm^{-1} (−CO−NH_2) which correspond to the absorbance of the sugar-phosphate backbone and nitrogenous base of oligonucleotide aptamer (Fig. 2C), similar to the NT-proBNP aptamer stock (Fig. 2A). Moreover, the characteristic peaks of a phosphate group in the sugar moiety of DNA in the lower wavenumber region (1250–500 cm^{-1}) are essentially due to the deoxyribose region of DNA [27]. Similarly, the complexes of NT-proBNP and aptamer were detected (−CO−NH; 3341, 1654, and 1557 cm^{-1}) and the region below 1000 cm^{-1} (Fig. 2D). There was also a peak (984 cm^{-1}) observed for the complexes of NT-proBNP and aptamer, which correspond to the absorbance of NT-proBNP protein

(Fig. 2B). Therefore, the presence of FTIR spectra demonstrated that the fabrication of NT-proBNP microelectrode array was successful assigned to the NH_2–Au coupling. However, the presence of captured NT-proBNP was not obviously observed regarding the extremely low amount of NT-proBNP analyte.

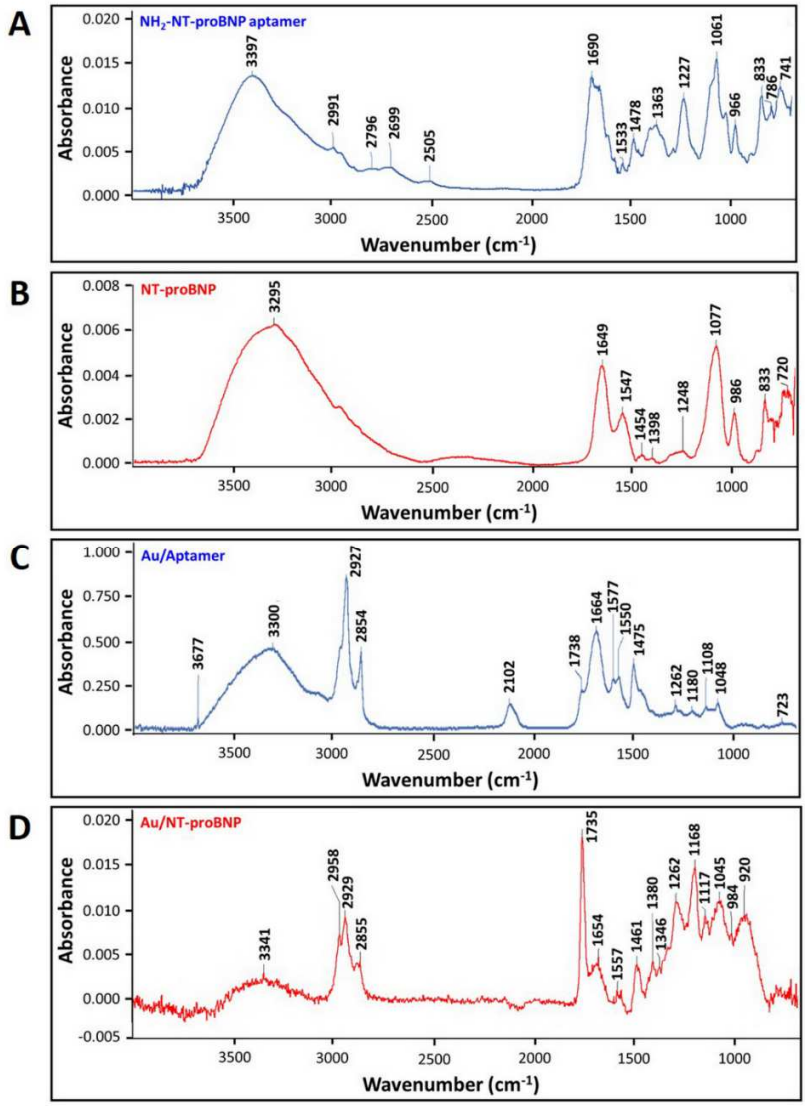

Fig. 2. FTIR spectroscopy confirmed the presence of NT-proBNP aptamer on the surface of modified Au microelectrode array. FTIR spectra of (A) NT-proBNP aptamer, (B) NT-proBNP protein, (C) Au/Aptamer (D) Au/Aptamer/NT-proBNP at 4000–500 cm^{-1}.

As shown in Fig. 3A, the measured contact angle of water droplet on freshly pretreated Au surface was 72° ± 1.71. After the NH_2-modified NT-proBNP aptamer deposition, the angle was lower than the bare Au (54° ± 1.15), indicating that the interaction between the Au surface and the aptamer is favorable. Similarly, the CAM of captured NT-proBNP by aptamer was 53° ± 2.27. The results concluded the high adhesion of NT-proBNP-aptamer complex onto the Au-functionalized surface. To confirm the NH_2-NT-proBNP aptamer was bound to the target NT-proBNP, fluorescence observation was further performed by. There was no fluorescence detectable when the microelectrode was fabricated without the incubation of NT-proBNP (Fig. 3B). As expected, the green fluorescent NT-proBNP was observed on the surface of fabricated microelectrode after being captured by the modified aptamer. To sum up, all of these characteristic finding proven by FTIR, CAM, and fluorescence spectroscopy indicates that NT-proBNP-aptamer was assembled successfully onto the Au microelectrode array.

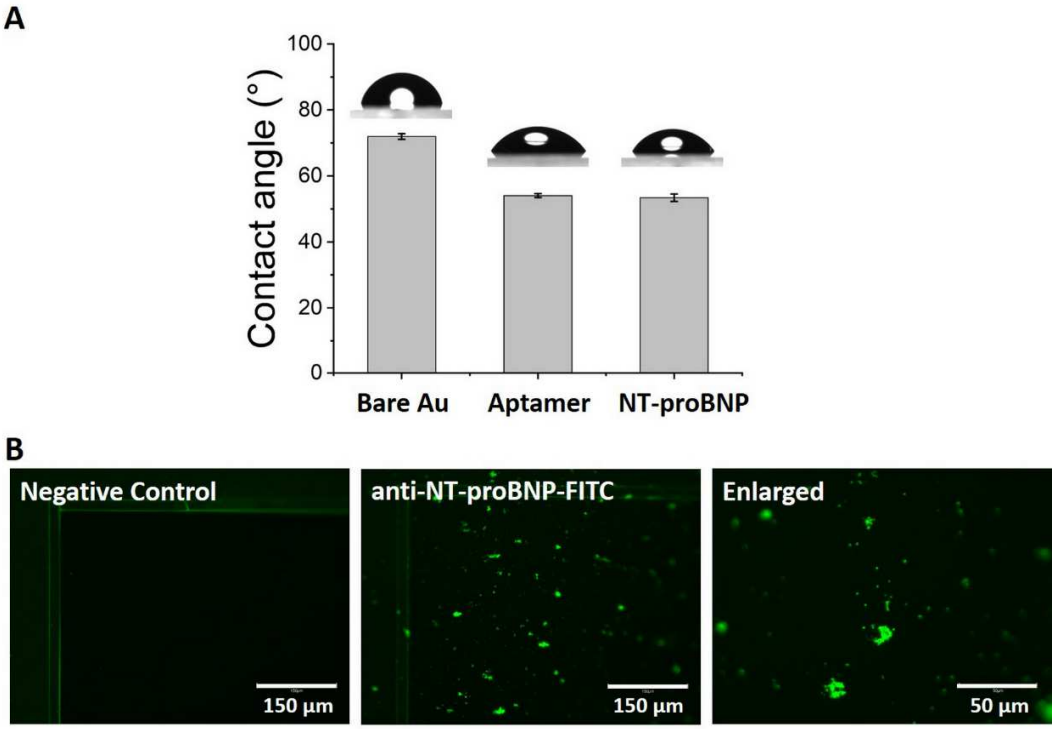

Fig. 3. (A) Detection of the boundary-layer effects in water droplet. The CAM was reproduced in quadruplicate and the error bar represents the standard error of the mean (SEM). (B) Fluorescence imaging of the NH_2-NT-proBNP aptamer on the Au surface when the aptamer was bound with NT-proBNP protein (magnification 20x and 60x, respectively).

3.2. Electrochemical biosensing performances of the NT-proBNP-based aptasensor

When the NT-proBNP aptamer strand immobilizes over Au surface of the microelectrode array, NT-proBNP molecules can be successfully recognized by a specific NT-proBNP aptamer binding event. As shown in Fig. 4A, a reversible cyclic voltammogram was obtained for bare microelectrodes (black line). The gold WEs were modified with coimmobilization of NH_2-modified NT-proBNP aptamer and MCH (red line). The peak-shaped voltammogram was smaller (ΔEp = 217.6 mV) than the bare one (ΔEp = 164.6 mV). The conductivity of the microelectrode surface was getting worse, owing to the electrostatic repulsion of negative-charged phosphate backbone of the aptamer and the redox probe as previously described [25]. Hereafter, the capture of NT-proBNP onto the modified microelectrode surface further decreased the peak-to-peak potential separation (blue line; ΔEp = 134.6 mV), caused by the conductivity of the electrode interface. The situation mentioned above was consistent with the resistance change on the WEs surface of microelectrodes (Fig. 4B). The bare microelectrodes presented a small semicircle in the EIS response with a low resistance value of 399.9 kΩ (black line), showing its excellent electrochemical conductivity and low electron transfer resistance.

Generally, immobilizing biomolecules by thiol group is a well-known technique for self-assembling monolayers on gold surfaces. In this experiment, aminated NT-proBNP aptamer can be attached to the gold surface of the biosensor regarding the substantial coordination of gold with the amine group [28]. Subsequently, MCH was coimmobilizated in order to block nonspecifically adsorbed

parts while ensuring a controlled vertical orientation of immobilized aptamers, by repulsing negatively charged OH terminus of MCH and DNA phosphate backbone [29]. After the immobilization of aptamer and MCH, the raised shape-liked semicircle was observed as a resistance value of 449.6 kΩ (red line), hinting the repulsion force of the introduced aptamer and $[Fe(CN)_6]^{3-/4-}$ and hampering the electron transfer on the electrode surface. Finally, the modified gold WEs was treated with NT-proBNP, and the diameter of the semicircle abruptly increased to 550.5 kΩ (blue line), correlating to the aptamer-protein complex and resulting in an electrochemical signal change. As shown above, the good performance of CV and EIS responses indicated that every step of the modification was successful due to electron transfer on the Au surface of the microelectrodes.

Moreover, the incubation time of the aptasensor was optimized to ensure the optimal binding reaction between the capture NT-proBNP aptamer and target NT-proBNP (Fig. 4C-D). The diameter of semicircle in the Nyquist plot gradually decreased from 15 to 30 min. This event could happen according to short-chain alkanethiols MCH which has been reported to exhibit fewer defects of gradual reorganization [29]. Therefore, the additional time of incubation with NT-proBNP negatively affects the adsorption and desorption charge transfer resistance of immobilized aptamers leading to impair target binding. A calibration curve representing the change in ΔR/R (ΔR/R = R, NT-proBNP detection – R, aptamer immobilization), and fitted linear regression equation as ΔR/R = 1.1669[NT-proBNP] + 3.1136 with an R^2 value of 0.9995 and ΔR/R = 0.0845[NT-proBNP] + 0.6033 with an R^2 value of 0.9710 for 15 min and 30 min, respectively. Thus, the incubation time of 15 min was chosen as the optimal value. Fig. 4E illustrates the Nyquist plots of the NT-proBNP-based aptasensor incubated with different concentrations. This result demonstrates that R values increase with increasing NT-proBNP concentration. A calibration curve representing the change in ΔR/R to various concentrations of NT-proBNP was in the range of $5.0x10^{-3}$ to 1.0 pg mL^{-1}, and fitted linear regression equation as ΔR/R =

1.17[NT-proBNP] + 2.88 with an R^2 value of 0.9624 (Fig. 4F). Particularly, the capabilities of the novel multi-microelectrode array can be possibly performed multiple tasks at the same time, allowing shorter analysis time, simultaneous operation for different analytes, and capability for repeated application.

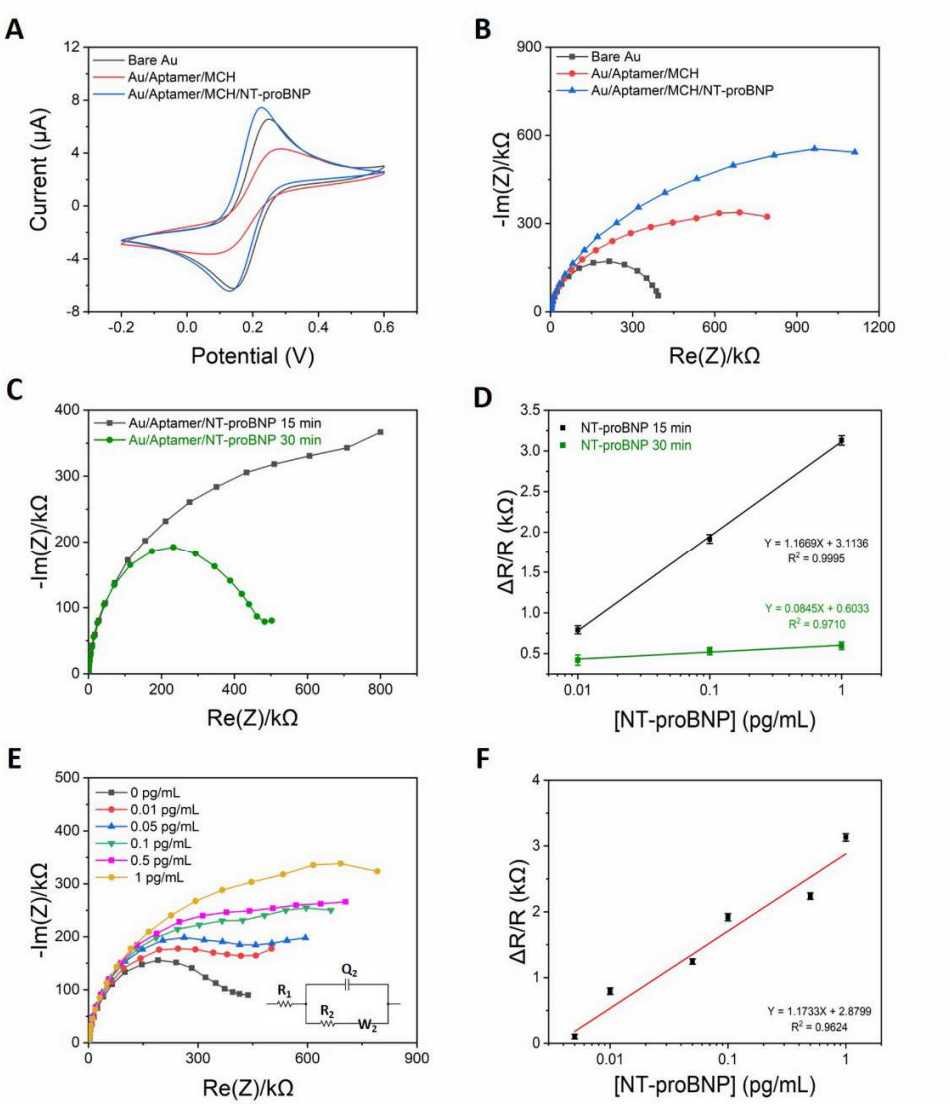

Fig. 4. (A) Cyclic voltammetry of the aptasensor showing an increase in the current and (B) Nyquist plots during the fabrication recorded in 5.0 mM $[Fe(CN)_6]^{3-/4-}$ redox probe. (C) Nyquist curves for the incubation time of NT-proBNP (D) Calibration curve for detecting the different time incubations on the charge transfer resistance (ΔR/R) of NT-proBNP. (E) Impedance spectra after deposition of NT-proBNP aptamer on microelectrode array that correspond to the various concentrations of NT-proBNP. (F)

Linear relationship between the ΔR/R and the NT-proBNP concentration. Error bars represent the SEM of the quadruplicates.

In order to verify specificity of the developed NT-proBNP microelectrode array, other proteins, including proBNP, IL-10, and TNF-alpha were used as possible interferences that are commonly present in saliva matrix as cardiac biomarkers. The same direct assay as a specific target (NT-proBNP) and change in ΔR/R with respect to aptamer-functionalized microelectrodes without any analyte was recorded. As shown in Fig. 5A, 1.0, 5.0, 10.0, and 20.0 pg mL^{-1} of interfering substances did not make any obvious changes in EIS response to the NT-proBNP aptasensor. The evaluated percent relative standard derivation (% RSD) for three independent electrodes of the obtained signals was less than 10% (Table S1). These results exhibited an excellent specificity for NT-proBNP. Under optimized conditions, reproducibility was determined by measuring the EIS response of NT-proBNP 1.0 pg mL^{-1} for four independent microelectrodes and represented as histograms and error bars, which showed an acceptable RSD (6.4%) of the ΔR/R, indicating that the constructed aptasensor possessed well-deserved reproducibility (Fig. 5B, Table S2). Towards this, long-term stability is one of the essential parameters to detect a possible signal of the analyte due to aging effects. The aptasensor was stored at 4 °C and measured at a fixed concentration of 1.0 pg mL^{-1} at the desired period. After two weeks of storage, the aptasensors highly retained a similar recovery of the initial response signal according to the stable aptamers conjugated to a linker self-assembled monolayer, which strengthened the immobilization of the modified aptamer onto the surface. The proposed NT-proBNP aptasensor revealed good satisfaction for maintaining its function and stability with an RSD of 0.8% (Fig. 5C, Table S3).

Moreover, an important challenge in biosensing technology is reusability which generates consistent identical responses and maintains its sensitivity by using a single sensor multiple times [30].

To regenerate the microelectrode array after each addition of NT-proBNP, 10.0 mM NaOH was employed due to its nucleic acid denaturant, allowing deform aptamer covalent bonding and release the NT-proBNP from the surface [31]. Briefly, the aptamer-NT-proBNP complexes were broken by 10.0 mM NaOH for 10 min and then incubated in PBS solution containing NT-proBNP. The interfacial electron-transfer resistances (ΔR/R) observed for the NT-proBNP aptamer-functionalized microelectrode were diminished after regeneration and the main EIS responses were reversed after the process. Reassociation has restored the increased relative ΔR/R. The cycle of capture, release, and analysis can be repeated at least four times at the same aptamer-functionalized microelectrode with no significant change in the microelectrode behavior (Fig. 5D, Table S4). This could be explained by the highly reproducible property of the aptamer [32]. Thus, the newly NT-proBNP aptasensor has a high level of reliability and efficiency.

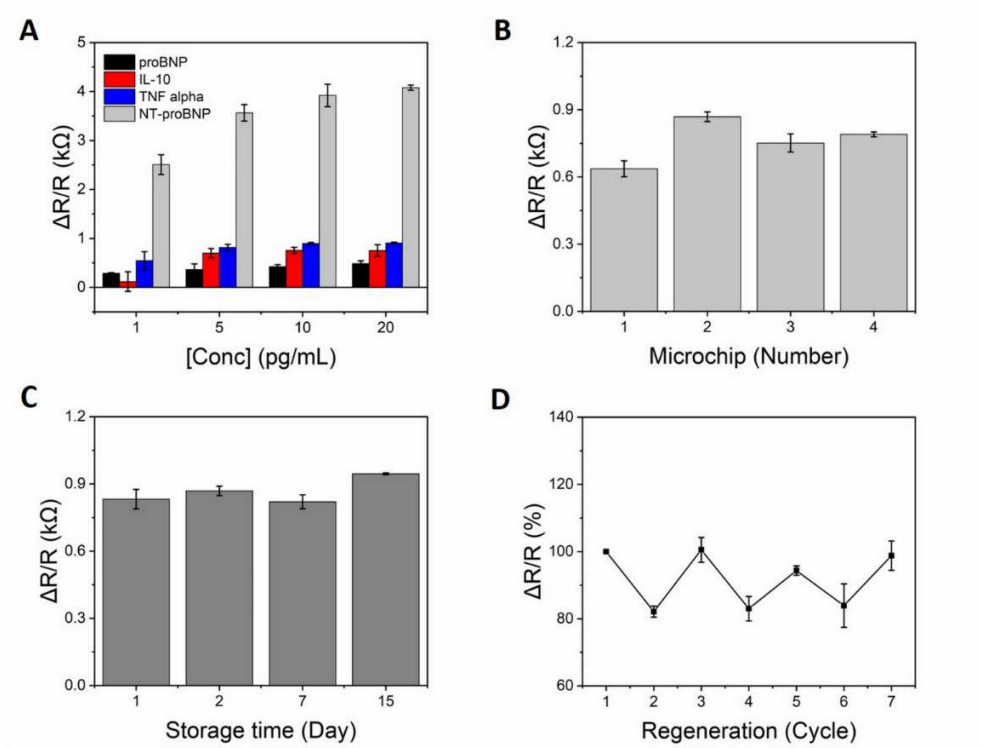

Fig. 5. EIS responses of the aptasensor to assess the sensing quality for the detection of NT-proBNP. (A) Specificity, (B) reproducibility, (C) long-term stability, and (D) sensor interrogation-regeneration plots were obtained. Error bars correspond to SEM of measurements obtained from three identical electrodes.

3.3. Practicability of the aptasensor toward NT-proBNP

Presently, blood is the most common sampling for clinical investigation. It is an invasive technique that usually concurs with early clotting and blood-borne infectious transmission. Therefore, saliva sampling is considered less complex biological matrices to overcome these disadvantages of blood sampling [33]. The similarities between saliva and plasma proteins along with the valuable role of NT-proBNP inspired us to validate the applicability of the NT-proBNP-based aptasensor which highlighted the diagnostic potential of artificial saliva. EIS responses were collected as corresponding binding signals and the recovery rates were obtained from four-independent microelectrodes, as summarized in Table 1. The recovery rates of all samples were found to be between 94.0 – 100.4%, suggesting high accuracy and remarkable feasibility of the fabricated aptasensor. These results were in agreement with the previous work presenting the NT-proBNP protein in human saliva samples by using an Immunologically Modified Field Effect Transistor (IMFET) with a LOD of $2x10^{-2}$ pg mL^{-1} [34]. Surprisingly, the aforementioned findings demonstrated that the half-life of NT-proBNP is longer than BNP up to 90 minutes, indicating a useful biomarker for the management of heart failure patients [35].

Table 1. Determination of NT-proBNP in artificial saliva.

Spiked NT-proBNP concentration (pg mL^{-1})	**Detected NT-proBNP concentration (pg mL^{-1})**	**Recovery (%)**
1	0.98 ± 0.03	98.0
2	1.88 ± 0.04	94.0
5	5.02 ± 0.02	100.4

In the case of a conventional enzyme-linked immunosorbent assay (ELISA) kit approved for diagnostic use in Europe, human serum and plasma samples were validated in the range of 85 – 5424 pg mL^{-1} with a limit of detection (LOD) of 25.4 pg mL^{-1} provided by the manufacturer. The quantitative measurement of NT-proBNP levels in saliva samples was further determined with 1.0 pg mL^{-1} of LOD [36]. Compared with the recently reported traditional ELISA kit and NT-proBNP aptasensors, the present microelectrode array displays a good linear relationship in the desired range of NT-proBNP concentration with a low LOD of $5x10^{-3}$ pg mL^{-1} (Table 2). This finding might be occurred due to the advantages of the aptamer-modified microelectrode surface over antibodies, including strong affinity, specific target binding, enhanced stability, easier immobilization, and higher reproducibility [37, 38]. Furthermore, integration with multiplexed potentiostat is the next step which will provide the parallel investigation with a larger amount of potential cardiac biomarkers in real clinical samples for further validation of the proposed microelectrode array. Particularly, the fully automated microfluidic system has been developed for next-generation point-of-care devices for rapid screening of cardiac aptamers in patient serum samples [39]. The advanced approach demonstrated here will offer rapid diagnosis, ease of implementation, simplicity, as well as affordability for the risk assessment and management of heart failure.

Table 2. Comparisons of different electrochemical aptasensors for NT-proBNP detection[a].

Method	Biorecognition	Strategy	Sample	Linear range (pg mL^{-1})	LOD (pg mL^{-1})	Ref
CL	MB-aptamer protein-Ab sandwich complexes	Glass-based microfluidic system	Serum	4.6 – $5x10^3$	1.5	[22]
EM	GNR	Si-based IDE	-	10.0 – $1x10^5$	1 .0	[40]
EM	ZEO-IO with biotin-streptavidin	Si-based integrated microsensor	Serum	10.0 – 32.0	1.0 – 2.0	[23]
EIS	NH_2-terminated aptamer-MCH	Au microchip	Artificial saliva	$5x10^{-3}$ – 1.0	$5x10^{-3}$	In this work

[a] CL, chemiluminescence; MB, magnetic bead; Ab, antibody; EM, electrical measurement; GNR, utilized gold nanorod; IDE, interdigitated electrode; ZEO-IO, zeolite-iron oxide nanocomposite; Si, silicon; EIS, electrochemical impedance spectroscopy; NH_2, amine; MCH, 6-Mercapto-1-hexanol; Au, gold

4. Conclusion

The novel approach for the fabrication of single-step impedimetric NT-proBNP aptasensor was successfully constructed for sensitively detecting NT-proBNP-related cardiac insufficiency protein. Over antibody-based biosensors and the conventional ELISA method, this sensor represents clear advantages including ease of preparation, fast response, robustness, and cost-effective fabrication, which may hold great potential in fields of cardiac insufficiency monitoring. The proposed NT-proBNP aptasensor not only possessed ultrasensitively with a LOD of $5x10^{-3}$ pg mL^{-1}, but also exhibited satisfactory selectivity, long-term stability, and high reproducibility. Consequently, the impedimetric data revealed the efficiency toward NT-proBNP, which is mainly attributed to outstanding stability of aptamer strands to strong binding affinity and charge electron transfer onto the gold metal surface enabled reusability without any significant loss in sensor sensitivity at least 4 regenerations.

CRediT authorship contribution statement

Waralee Ruankham: methodology, investigation, formal analysis, original draft, review and editing, funding acquisition. **Isaac Aarón Morales Frías:** methodology, investigation. **Kamonrat Phopin:** conceptualization, review and editing, funding acquisition. **Tanawut Tantimongcolwat:** conceptualization, review and editing, funding acquisition. **Joan Bausells:** methodology. **Nadia Zine:** review and editing, supervision. **Abdelhamid Errachid:** conceptualization, methodology, formal analysis, review and editing, supervision, funding acquisition.

Declaration of competing interest

The authors declare that they have no known competing financial interests or personal relationships that could have appeared to influence the work reported in this paper.

Acknowledgements

This work was financially supported by the Franco-Thai Cooperation Programme in Higher Education and Research/Franco-Thai Mobility Programme/PHC SIAM 2020-2021; the POC4allergies project from ERA PerMed ERA-NET [grant number 768686]; and the Bionanosens project from the European Union's Horizon 2020 [grant number 951887].

References

[1] G. Lippi, F. Sanchis-Gomar, Global epidemiology and future trends of heart failure, AME Med J, 5(2020) 15. https://doi.org/10.21037/amj.2020.03.03

[2] N.L. Bragazzi, W. Zhong, J. Shu, A. Abu Much, D. Lotan, A. Grupper, et al., Burden of heart failure and underlying causes in 195 countries and territories from 1990 to 2017, Eur J Prev Cardiol, 28(2021) 1682-90. https://doi.org/10.1093/eurjpc/zwaa147%J

[3] A. Groenewegen, F.H. Rutten, A. Mosterd, A.W. Hoes, Epidemiology of heart failure, Eur J Heart Fail, 22(2020) 1342-56. https://doi.org/10.1002/ejhf.1858

[4] G. Savarese, L.H. Lund, Global public health burden of heart failure, Card Fail Rev, 3(2017) 7-11. https://doi.org/10.15420/cfr.2016:25:2

[5] V.L. Roger, Epidemiology of heart failure, Circ Res, 128(2021) 1421-34. https://doi:10.1161/CIRCRESAHA.121.318172

[6] V. Castiglione, A. Aimo, G. Vergaro, L. Saccaro, C. Passino, M. Emdin, Biomarkers for the diagnosis and management of heart failure, Heart Fail Rev 27(2022) 625-43. https://doi.org/10.1007/s10741-021-10105-w

[7] N.E. Ibrahim, J.L. Januzzi, Established and emerging roles of biomarkers in heart failure, Circ Res, 123(2018) 614-29. https://doi.org/10.1161/CIRCRESAHA.118.312706

[8] C. Mueller, K. McDonald, R.A. de Boer, A. Maisel, J.G.F. Cleland, N. Kozhuharov, et al., Heart Failure Association of the European Society of Cardiology practical guidance on the use of natriuretic peptide concentrations, Eur J Heart Fail, 21(2019) 715-31. https://doi.org/10.1002/ejhf.1494

[9] Y. Peng, N. Raj, J.W. Strasser, R.M. Crooks, Paper biosensor for the detection of NT-proBNP using silver nanodisks as electrochemical labels, Nanomaterials (Basel), 12(2022) 2254. https://doi.org/10.3390/nano12132254

[10] R.D. Crapnell, N.C. Dempsey, E. Sigley, A. Tridente, C.E. Banks, Electroanalytical point-of-care detection of gold standard and emerging cardiac biomarkers for stratification and monitoring in

intensive care medicine - A review, Microchim Acta, 189(2022) 142. https://doi.org/10.1007/s00604-022-05186-9

[11] H. Alawieh, T.E. Chemaly, S. Alam, M. Khraiche, Towards point-of-care heart failure diagnostic platforms: BNP and NT-proBNP biosensors, Sensors (Basel), 19(2019) 5003. https://doi.org/10.3390/s19225003

[12] V. Mani, C. Durmus, W. Khushaim, D.C. Ferreira, S. Timur, F. Arduini, et al., Multiplexed sensing techniques for cardiovascular disease biomarkers - A review, Biosens Bioelectron, 216(2022) 114680. https://doi.org/10.1016/j.bios.2022.114680

[13] Y. Ning, J. Hu, F. Lu, Aptamers used for biosensors and targeted therapy, Biomed Pharmacother, 132(2020) 110902. https://doi.org/10.1016/j.biopha.2020.110902

[14] L.A. Stanciu, Q. Wei, A.K. Barui, N. Mohammad, Recent advances in aptamer-based biosensors for global health applications, Annu Rev Biomed Eng, 23(2021) 433-59. https://doi.org/10.1146/annurev-bioeng-082020-035644

[15] G. Cai, Z. Yu, R. Ren, D. Tang, Exciton-plasmon interaction between AuNPs/graphene nanohybrids and CdS quantum dots/TiO(2) for photoelectrochemical aptasensing of prostate-specific antigen, ACS Sens, 3(2018) 632-9. https://doi.org/10.1021/acssensors.7b00899

[16] Z. Qiu, J. Shu, J. Liu, D. Tang, Dual-channel photoelectrochemical ratiometric aptasensor with up-converting nanocrystals using spatial-resolved technique on homemade 3D printed device, Anal Chem, 91(2019) 1260-8. https://doi.org/10.1021/acs.analchem.8b05455

[17] Z. Qiu, J. Shu, D. Tang, Near-infrared-to-ultraviolet light-mediated photoelectrochemical aptasensing platform for cancer biomarker based on core-shell NaYF(4):Yb,Tm@TiO(2) upconversion microrods, Anal Chem, 90(2018) 1021-8. https://doi.org/10.1021/acs.analchem.7b04479

[18] Z. Qiu, J. Shu, D. Tang, Bioresponsive release system for visual fluorescence detection of carcinoembryonic antigen from mesoporous silica nanocontainers mediated optical color on quantum dot-enzyme-impregnated paper, Anal Chem, 89(2017) 5152-60. https://doi.org/10.1021/acs.analchem.7b00989

[19] Z. Li, M.A. Mohamed, A.M. Vinu Mohan, Z. Zhu, V. Sharma, G.K. Mishra, et al., Application of electrochemical aptasensors toward clinical diagnostics, food, and environmental monitoring: Review, Sensors (Basel, Switzerland), 19(2019) 5435. https://doi.org/10.3390/s19245435

[20] M. Majdinasab, J.L. Marty, Recent advances in electrochemical aptasensors for detection of biomarkers, Pharmaceuticals (Basel, Switzerland), 15(2022) 995. https://doi.org/10.3390/ph15080995

[21] R. Abd-Ellatief, M.R. Abd-Ellatief, Electrochemical aptasensors: Current status and future perspectives, Diagnostics (Basel, Switzerland), 11(2021) 104. https://doi.org/10.3390/diagnostics11010104

[22] A. Sinha, P. Gopinathan, Y.-D. Chung, S.-C. Shiesh, G.-B. Lee, Simultaneous detection of multiple NT-proBNP clinical samples utilizing an aptamer-based sandwich assay on an integrated microfluidic system, Lab Chip 19(2019) 1676-85. https://doi.org/10.1039/C9LC00115H

[23] Z. Liu, S.C.B. Gopinath, Z. Wang, Y. Li, P. Anbu, W. Zhang, Zeolite-iron oxide nanocomposite from fly ash formed a 'clubbell' structure: Integration of cardiac biocapture macromolecules in serum on microelectrodes, Mikrochim Acta, 188(2021) 187. https://doi.org/10.1007/s00604-021-04834-w

[24] A. Sinha, P. Gopinathan, Y.D. Chung, H.Y. Lin, K.H. Li, H.P. Ma, et al., An integrated microfluidic platform to perform uninterrupted SELEX cycles to screen affinity reagents specific to cardiovascular biomarkers, Biosens Bioelectron, 122(2018) 104-12. https://doi.org/10.1016/j.bios.2018.09.040

[25] W. Ruankham, T. Tantimongcolwat, K. Phopin, J. Bausells, M. Hangouët, M. Martin, et al., Split aptamers immobilized array microelectrodes for detection of chlorpyrifos pesticide using electrochemical impedance spectroscopy, Sen Actuators B Chem, 372(2022) 132614. https://doi.org/10.1016/j.snb.2022.132614

[26] F.G. Bellagambi, A. Baraket, A. Longo, M. Vatteroni, N. Zine, J. Bausells, et al., Electrochemical biosensor platform for TNF-α cytokines detection in both artificial and human saliva: Heart failure, Sens Actuators B Chem, 251(2017) 1026-33. https://doi.org/10.1016/j.snb.2017.05.169

[27] A.W. Parker, S.J. Quinn, Infrared Spectroscopy of DNA, in: G.C.K. Roberts (Ed.) Encyclopedia of Biophysics, Springer Berlin Heidelberg, Berlin, Heidelberg, 2013, pp. 1065-74. https://doi.org/10.1007/978-3-642-16712-6_112

[28] D.J. Dunaway, R.L. McCarley, Scanning force microscopy studies of enhanced metal nucleation: Au vapor deposited on self-assembled monolayers of substituted silanes, Langmuir, 10(1994) 3598-606. https://doi.org/10.1021/la00022a037

[29] F.V. Oberhaus, D. Frense, D. Beckmann, Immobilization techniques for aptamers on gold electrodes for the electrochemical detection of proteins: A review, Biosensors (Basel), 10(2020) 45. https://doi.org/10.3390/bios10050045

[30] J.A. Goode, J.V.H. Rushworth, P.A. Millner, Biosensor regeneration: A review of common techniques and outcomes, Langmuir, 31(2015) 6267-76. https://doi.org/10.1021/la503533g

[31] L.H. Lauridsen, H.A. Shamaileh, S.L. Edwards, E. Taran, R.N. Veedu, Rapid single-step selection method for generating nucleic acid aptamers: Development of a DNA aptamer against α-bungarotoxin, PLoS One, 7(2012) e41702. https://doi.org/10.1371/journal.pone.0041702

[32] M.A. Morales, J.M. Halpern, Guide to selecting a biorecognition element for biosensors, Bioconjugate Chem, 29(2018) 3231-9. https://doi.org/10.1021/acs.bioconjchem.8b00592

[33] A. Joharimoghadam, M. Tajdini, A. Bozorgi, Salivary B-type natriuretic peptide: A new method for heart failure diagnosis and follow-up, Kardiol Pol, 75(2017) 71-7. https://doi.org/10.5603/KP.a2016.0097

[34] H. Ben Halima, F.G. Bellagambi, M. Hangouët, A. Alcacer, N. Pfeiffer, A. Heuberger, et al., A novel electrochemical strategy for NT-proBNP detection using IMFET for monitoring heart failure by saliva analysis, Talanta, 251(2023) 123759. https://doi.org/10.1016/j.talanta.2022.123759

[35] J.Y. Foo, Y. Wan, K. Kostner, A. Arivalagan, J. Atherton, J. Cooper-White, et al., NT-ProBNP levels in saliva and its clinical relevance to heart failure, PLoS One, 7(2012) e48452. https://doi.org/10.1371/journal.pone.0048452

[36] F.G. Bellagambi, C. Petersen, P. Salvo, S. Ghimenti, M. Franzini, D. Biagini, et al., Determination and stability of N-terminal pro-brain natriuretic peptide in saliva samples for monitoring heart failure, Scientific reports, 11(2021) 13088. https://doi.org/10.1038/s41598-021-92488-2

[37] S. Arshavsky-Graham, C. Heuer, X. Jiang, E. Segal, Aptasensors versus immunosensors—Which will prevail?, Eng Life Sci, 22(2022) 319-33. https://doi.org/10.1002/elsc.202100148

[38] M. Prante, E. Segal, T. Scheper, J. Bahnemann, J. Walter, Aptasensors for point-of-care detection of small molecules, Biosensors (Basel), 10(2020) 108. https://doi.org/10.3390/bios10090108

[39] A. Sinha, T.-Y. Tai, K.-H. Li, P. Gopinathan, Y.-D. Chung, I. Sarangadharan, et al., An integrated microfluidic system with field-effect-transistor sensor arrays for detecting multiple cardiovascular biomarkers from clinical samples, Biosens Bioelectron 129(2019) 155-63. https://doi.org/10.1016/j.bios.2019.01.001

[40] C. Qiu, X. Wang, X. Zhang, Z. Li, Y. Zhou, J. Kang, Sensitive determination of NT-proBNP for diagnosing abdominal aortic aneurysms incidence on interdigitated electrode sensor, Biotechnol Appl Biochem, 68(2021) 865-70. https://doi.org/10.1002/bab.2006

Graphical abstract